International Journal of Engineering Trends and Technology
ISSN: 2231 – 5381 /doi:10.14445/22315381/IJETT-V68I11P219
Volume 68 Issue 11, 145-149, November 2020

Numerical modeling and experimental validation of new energetic materials in favor of photovoltaic modules

Khadija Ezzouitine [#1], Mustapha Jammoukh [*2], Abdelilah Hachim [#3], Abdelkader Boulezhar [#4]

[1-4] *Laboratory of renewable energy and dynamic of systems University Hassan II, Faculty of Sciences Ain-Chock Casablanca, Morocco*
[2] *Laboratory of Signals, Distributed systems and Artificial Intelligence (SSDIA), Hassan II University of Casablanca, Higher Normal School of Technical Education, P.O. Box 159 28 820 Mohammedia, Morocco. 3[2] [3]Université Hassan II-Casablanca (UH2C), Ecole nationale supérieure d'électricité et de mécanique laboratoire contrôle et caractérisation mécanique des matériaux et des structure, Casablanca, Maroc*
Institut Supérieur d'Etudes Maritimes (ISEM), Km 7, Route d'El Jadida Casablanca

[1] khadija.ezzouitine@gmail.com, [2]jamoukh@yahoo.fr, [3]abdelilah.hachim@gmail.com [4] boulezhara@gmail.com

***Abstract* —** *A photovoltaic module consists of grouping photovoltaic cells in series or parallel to allow their use at practical voltages and currents while ensuring their electrical insulation and their protection against external factors as humidity, rain, snow, etc. dust, corrosion, or mechanical shock.*
In this perspective, we plan to establish a numerical Modeling and experimental validation of new material such as S355 steel in favor of photovoltaic panels' framework given its energy potential.
To this end, our work will be focused on numerical modeling by finite elements of a double notch tensile test specimen using the CAST3M 2009 calculation code. We will analyze the evolution of the maximum stress along the axis of the l. test specimen and the stress concentration factor with the crack length and the applied stress.

Keywords — *Notch, finite elements, photovoltaic, maximum stress, stress concentration factor, nominal stress.*

I. INTRODUCTION

In metal structures, cracks most often begin at the level of geometric discontinuities such as notch (defects). The geometric parameters of the structures and discontinuities govern the priming or propagation of cracks and, therefore, the holding in the structural resistance service. In the industrial sector, for economic or safety reasons, we try to know the degree of harmfulness of these defects and their residual lifespan. This involves establishing models based on the mechanics of rupture or fatigue. In terms of defects, the distribution of stresses is relatively complex, as are fracture mechanics parameters. Digital methods, such as finished elements, provide a robust solution to this problem. This solution must be validated, compared to the analytical solution when it exists, and if possible, faced with experience. [Figure 1].

Fig. 1 solar panel Aluminium Frame

A. EL Hakimi [1] studied the correction function i0 by applying constant pressure along the crack's lips. According to the calculations' results, the integral J in the case of a defect at the base of the transition is always higher than that of a similar case in a straight tube [2].

II. METHOD USED

In this work, we consider a double-notch specimen side, stressed in tension (mode I), causing a crack opening. Finite elements discredited the specimen.

The simulation is done using the computer code CASTEM 2009, including a calculation procedure described in steps of calculation described by a specific code. The results are validated by the bibliographic results [3]. The applied stresses are Δσ: 352 MPa, 282MPa, and 248MPa.

The finite element method used in this report is suitable for the calculation of fracture mechanics. The area of the notch is finely refined.

The parameters to calculate the 3-dimensional geometric elements are cubic with 8 node elements.

Numerical calculations in fracture mechanics can generate large sequences. This may cause an inability to

solve these problems by means of a conventional computer or get erroneous results. Model validation is established by comparisons with other authors' numerical results; in cases where we have the analytical solution is compared with experimental results.

To validate our numerical results, we conducted a comparison with experimental results [3].

The study shows that the type of elements, the number of circles on the cut, and the mesh size directly affect calculation results.

III. EXPERIMENTAL SPECIMEN

The dimensions of notched tensile doubles specimens in S355 are shown in Figure 2 [3]. The section after machining these specimens is 221.9 mm2.

The tricky part of this operation is to achieve a root radius notch sharpest possible, to initiate a fatigue crack at low stresses.

The machining process using slitting saws was executed in several phases. Machining with a roughing cutter of the V-shaped notch. This produces a flat bottomed notch about 0.5 mm. Finishing the notch root with a well-sharpened cutter to fit the angle of 60°. The radius is less than 0.1 mm.

The microscope verifies the notch root radius at a magnification of 280. The cuts have obtained a radius of about 0.05mm.

TABLE 1. MECHANICAL PROPERTIES OF STEEL S355

Specification	Properties		
	σu (Mpa)	**σe (Mpa)**	**E (Gpa)**
S355	621	372	200

σu: Stress at break
σe: yield
E: Young's modulus

Its chemical composition is reported in Table 2.

TABLE 2. CHEMICAL COMPOSITION OF STEEL S355

	Composition (%)					
S355	**C**	**Mn**	**P**	**S**	**Si**	**Cu**
	0,29	0,80-1,20	0,09	0,05	0,15-0,30	0,20

A. Material

The material in our computer code is the Steel S355 (EN 10020). Its mechanical characteristics are summarized in Table 1.

Figure 3 shows the curve of conventional experimental evolution of the stress as a function of material deformation. The general shape of this curve showed a ductile behavior.

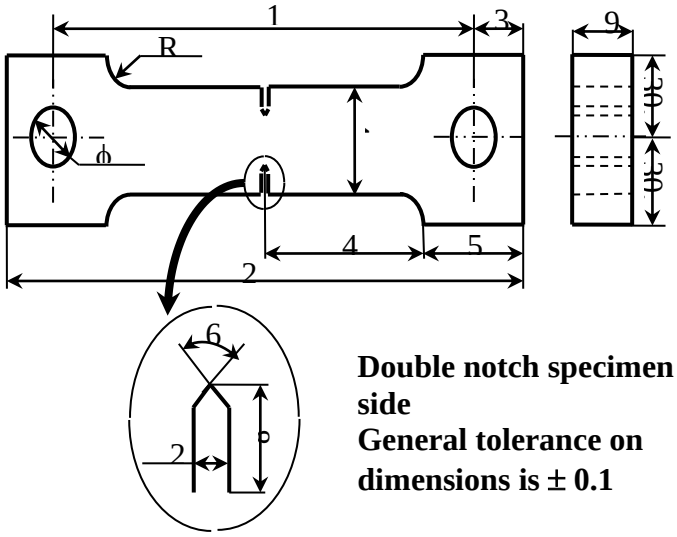

Fig. 2 Specimen dimensions of study

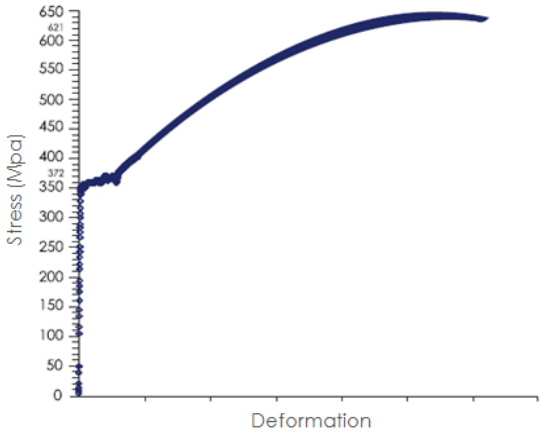

Fig. 3. Diagram of traction

Values main mechanical characteristics of the material obtained by tensile tests are given in Table 1.

B. Mesh and boundary conditions

In this section, we model the traction behavior of the bi-notched test tube. This problem has two symmetry planes, and therefore only a quarter of the test tube is Modeled. The model has 4980 cubic-type elements at 8 knots.

The mesh of the specimen is shown in Figure 4a. The mesh is refined notch root (Figure 4b).

The tensile force is applied to the specimen via a rigid triangle indicated by the arrow. This ensures that the effort is perfectly aligned.

From both sides of axes, the quarter of the sample studied's symmetry, and we inhibited all displacements and rotations U = 0 and R = 0.

IV. RESULTS AND DISCUSSION

A. Maximum stress and nominal stress traction

For an amplitude of applied stress Δσ, there is maximum stress and stress distribution along the traction axis. This axis is perpendicular to tensile stress and from the bottom of the notch until mid-width (half-ligament). In all cases, we verify that the maximum stress is located in σ_{Max} notch root.

This constraint then a parabolic evolution along the ligament to stabilize the value of nominal stress σnom.

Table 3 below gives the values of maximum stresses, ratings for the three levels of applied loads.

TABLE 3. NUMERICAL VALUES OF THE MAXIMUM STRESS AND THE NOMINAL STRESS WITH APPLIED STRESS

Δσ(MPa)	σMax(MPa)	σnom (MPa)
352	700	155
282	690	153
248	678	150

Δσ: stress applied
σMax: maximum stress
σnom: nominal stress
We note that the maximum stress and the nominal stress increases with applied stress.

B. Coefficient of stress digital concentration

Most structures are broken in the areas of stress concentration. These areas generally have either discontinuities or irregularities in the part's geometry (cuts, cracks ...). The notch root radius ρ increases with decreasing Kt for CT specimens, which tends to 0 as tends to infinity [3]. R. Peterson [4] defines the stress concentration factor Kt by:

$$Kt = \sigma max / \sigma nom \qquad (1)$$

We calculated the coefficient of dialogue constraint numerically from relation (1).

Table 4 below gives the values of maximum stresses, nominal, and the coefficients of stress concentration Kt three levels of applied loads.

TABLE 4. NUMERICAL VALUES OF MAXIMUM STRESS AND NOMINAL STRESS WITH APPLIED STRESS AND COEFFICIENT OF STRESS CONCENTRATION

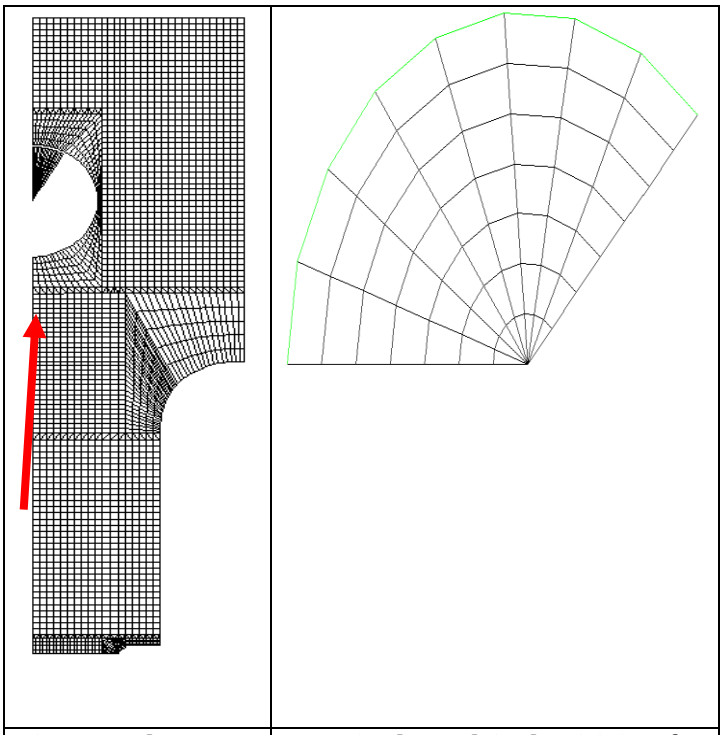

Fig 4a. Mesh | **Fig 4b. Mesh in the vicinity of the notch**

Δσ: stress applied
σ_{Max}: maximum stress
σnom: nominal stress
Kt (num): coefficients of stress digital concentration
Kt (exp): coefficients of experimental stress concentration

The numerical value of the stress concentration Kt coefficient for each of the three applied stresses (Δσ = 352 MPa, 282MPa, 248MPa) coincides with Kt found experimentally that its value is equal to 5 [3]. The small value of the notch radius (<0.2 mm) and its 60 ° angle make the stress concentration factor Kt high.

C. Evolution of numerical constraint along the horizontal axis of the specimen

The curves in Figure 5,6,7 show the evolution of numerical constraint along the specimen's horizontal axis for three stresses: Δσ = 352MPa, 282MPa, 248 MPa.

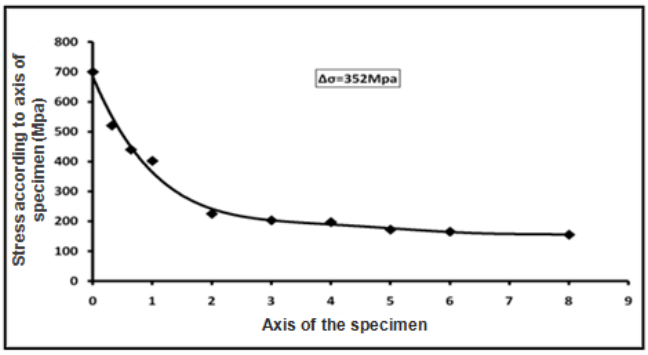

Fig 5. Evolution of numerical constraint along the horizontal axis of specimen for the applied stress Δσ = 352MPa

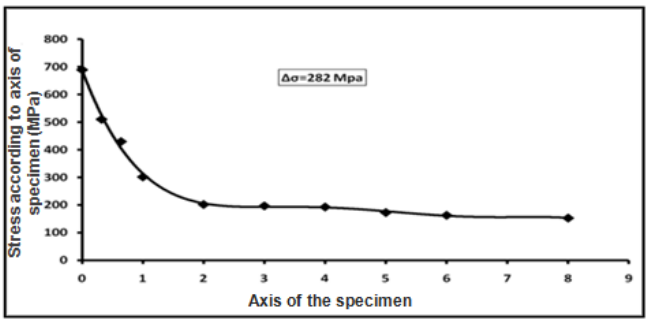

Fig 6. Evolution of numerical constraint along a horizontal axis of specimen for the applied stress Δσ = 282MPa

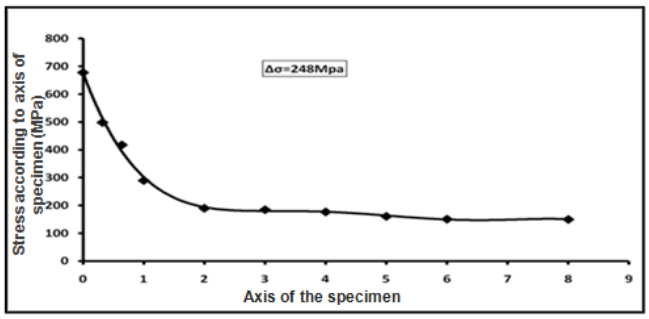

Fig 7. Evolution of numerical constraint along the horizontal axis of specimen for the applied stress Δσ = 248MPa

The numerical study reveals that maximum stress σMax is localized near the notch root for all three cases. This constraint to a parabolic trend over the range 0 to 2 mm to stabilize the value of nominal stress σnom. The maximum value is due to localized plastic flow. The notch vicinity's stress concentration causes plastic deformation in that area, while areas remote from the notch undergo only purely elastic deformation.

D. Evolution of the variation of stress concentration factor as a function of the digital length of the crack

Figure 8,9,10 shows the evolution of the various stress concentration factor as a function of crack length for the three applied stresses (Δσ = 352MPa, 282MPa, 248MPa).

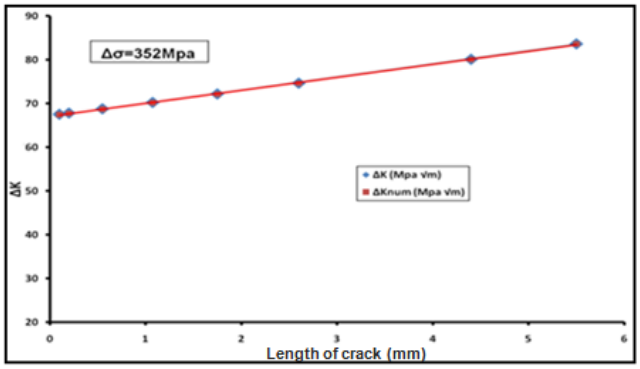

Fig 8. Evolution of variation stress concentration factor as a function of crack length for the applied stress Δσ = 352MPa

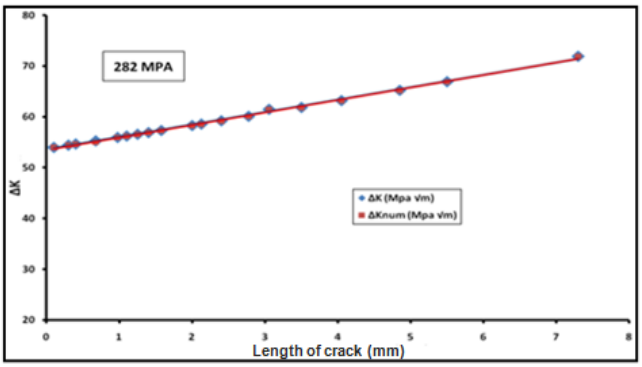

Fig 9. Evolution of variation stress concentration factor as a function of crack length for the applied stress Δσ = 282MPa

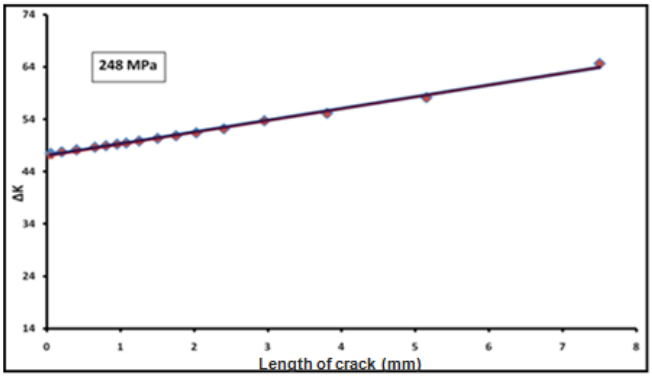

Fig 10. Evolution of variation stress concentration factor as a function of crack length for the applied stress Δσ = 248MPa

ΔK: variation of stress intensity factor (MPa √ m)

The comparison between the values of variation of stress concentration factor calculated by our model and literature [12] shows very good agreement, which allows it to validate our numerical model.

The analysis of curves of figure 5 shows a significant increase in the concentration factor as a function of the forced length of the crack and the applied stress.

V. CONCLUSION

In this study, the harmfulness of defects and nicks in cylindrical shells and pressure test tubes was apprehended, with a particular interest in the problem of nicks in notched test tubes.

This study used several branches of mechanics ranging from the mechanics of the rupture and the method of the finished elements that have become unavoidable given its power for solving complex problems, hence our approach's integrity

Digital modeling by finished elements was approached using Cast3m2009 software in the first place. A test tube with double cuts in S355 Steel was considered when used in traction, causing the crack to open with two symmetry planes, and therefore only a quarter of the test tube was modeled. The refinement of the mesh is carried out at the bottom of the notch using the Barsoum elements. The matching of numerical values obtained with experimental values allows us to validate our numerical study.

REFERENCES

[1] A. El Hakimi, Numerical and experimental study of the harmfulness of defects in cylindrical and spherical shells under pressure, Ph.D. The Thesis University of Technology of Compiègne, June 30, 2006.

[2] A. Saffih, S. Hariri, Numerical study of elliptical cracks in cylinders with a thickness transition, International Journal of Pressure Vessels and Piping, 83(1) (2006) 35-41.

[3] EL Ghorba M., Evolution of the damage and crack propagation under cyclic loading of A36 steel and aluminum 6351-T6, Memory Master and applied science, the University of Montreal in 1985.

[4] L. Niu, Study of the stress field of a plate having a V-notch with different acuities and implementation measures of the toughness of brittle materials, thesis, University of Metz, 1994.

[5] R. Peterson E., stress concentration factor, Jhon Wiley and Son New York, 1974.

[6] A. Hachim, EL Ghorba M., A. Akef, M. Chergui, The evolution of the stress intensity, stress concentration and cracking under cyclic loading for A36 steel and aluminum 6351 - T6, 9th Congress of Mechanics, Marrakech (2009) 21-24.

[7] A. Hachim, H. Farid, EL Ghorba M., M. Chergui, A. Akef, S. Hariri, Prediction and evolution of the fatigue crack initiation by the probabilistic method of A36 steel subjected to cyclic loading with constant amplitude (low cycle), VIèmes Days of Technical Studies in 2010, Marrakech – Morocco.

[8] BC Pinheiro. Pasqualino IP., Fatigue analysis of damaged steel pipelines Under cyclic internal pressure, Int J Fatigue 31 (2009) 962-73.

[9] A. Carpinteri, R. Brighenti, S. Vantadori, Notched double-curvature shells with cracks Under pulsating internal pressure, Int J Pressure Vessels Pip (2009) 1-11.

[10] A. Meksem, Probabilistic Approach and Experimental Characterization of Fatigue Behavior of Metallic Cable Lifting, Ph.D., ENSEM, 2010.

[11] A. Safih, Study of the harmfulness of crack in a cylinder with a thickness transition compared to a straight cylinder, Ph.D. Thesis University of Science and Technology of Lille, 2003.

[12] TH Topper, H. Haddad, Fatigue strength prediction of notches based on fracture Thresholds, 1st Int. Conf, Stockholm, 2, EMAS, Warley, UK, (1981) 777 to 797.

[13] Rahman, Brust, Approximate methods for predicting J-integral of a circumferentially surface cracked pipe subject to bending, International Journal of Fracture, 85 (1997) 111-130.

[14] P. Rabbe, The fatigue crack initiation, Fatigue of Materials and Structures, Paris Publisher Maloine SA and The University Press of Montreal Quebec (1980) 71-105.

[15] De Jésus AMP, Matos R, Fontoura BFC, Rebelo C, Sim˜oes Da Silva L, Veljkovic MA. Comparaison de le fatigue comportement entre S355 et S690 acier grades. J Constr Acier Res 79: (2012) 140-50.

[16] Haurant, P, Ménézo, C et réupeyrat, P, The PHOTOTHERM Project: Full Scale Experimentation and Modeling of a Photovoltaïque - Thermique (PV-T) Système hybride pour les applications d'eau chaude domestique, Energy Procedia, 48, (2014) 581,-587. 02/0903/0904/0905/0906/0907/090200400Ppv [W] SimulatedMeasured.

[17] Wanzhu Cai, Xiong Gong, Yong Cao Cellules solaires polymères: développement récent et voies possibles d'amélioration de til performance. Cellules Sol Energy Mater Sol 94: (2010) 114-127.

[18] Pawliczek, R., Prazmowski, M., Etude sur les changements de propriétés matérielles de mild acier S355 causé par des charges de bloc avec des contraintes moyennes variables, Journal international de fatigue. 80,(2015) 171-177.

[19] Lewandowski, J., Rozumek, D., 2016, Croissance de fissures dans l'acier S355 sous pliage cyclique avec joint soudé d'angle, théorique et appliqué Mécanique des fractures. 86, (2016) 342-350.

[20] Seitl S., Miarka P., Klusák J., Fintová S., Kunz L., Comparaison des taux de propagation des fissures par fatigue dans les aciers S355 J0 et S355 J2 Grades. Key Eng. Mater. 784,(2018) 91 -96.

[21] Seitl, S., Miarka, P., Klusák, J., Kala, Z., Krejsa, M., Blasón, S., Canteli, A a, Évaluation des propriétés de fatigue de l'acier S355 J0 à l'aide de Logiciel ProFatigue et ProPagation, Procedia Structural Integrity 13, (2018) 1494-1501.

[22] Wysokowski, A., 2018, Recherche sur les changements dans les propriétés du steel de l'ancien pont routier, Journal of Constructional Steel Research 147 (2018) 360–366.

[23] Wanzhu Cai, Xiong Gong, Yong Cao Cellules solaires polymères: développement récent et voies possibles d'amélioration de til performance. Cellules Sol Energy Mater Sol 94: (2010) 114-12.

[24] Pode R, Diouf B Éclairage solaire, énergie verte et technologie. Springer, Berlin / Heidelberg. doi: 10.1007 / 978-1-4471-2134-3_2 [5] (2011) https://slideplayer.com/slide/10702073/.

[25] De Jesus, AMP; Matos, R .; Fontoura, BFC; Rebelo, C.; Simões da Silva, L .; Veljkovic, M. Une comparaison de la fatigue behavior entre s355 et les nuances d'acier s690. J. Construct. Steel Res. 79 (2012) 140–150.

[26] De Jésus AMP, Matos R, Fontoura BFC, Rebelo C, Sim˜oes Da Silva L, Veljkovic MA. Comparaison de le fatigue comportement entre S355 et S690 acier grades. J Constr Acier Res 79:(2012) 140-50.https://doi.org/10.1016/j.jcsr.2012.07.021.